The American Journal of Pathology, Vol. 185, No. 5, May 2015

The American Journal of
PATHOLOGY
ajp.amjpathol.org

TUMORIGENESIS AND NEOPLASTIC PROGRESSION

Type III Collagen Directs Stromal Organization and Limits Metastasis in a Murine Model of Breast Cancer

Becky K. Brisson,* Elizabeth A. Mauldin,† Weiwei Lei,* Laurie K. Vogel,* Ashley M. Power,* Albert Lo,‡ Derek Dopkin,* Chand Khanna,§ Rebecca G. Wells,¶ Ellen Puré,‡ and Susan W. Volk*

From the Departments of Clinical Studies-Philadelphia, Pathobiology,† and Animal Biology,‡ School of Veterinary Medicine, and the Department of Medicine,¶ Perelman School of Medicine, University of Pennsylvania, Philadelphia, Pennsylvania; and the Tumor and Metastasis Biology Section,§ Pediatric Oncology Branch, Center for Cancer Research, National Cancer Institute, National Institutes of Health, Bethesda, Maryland*

Accepted for publication January 22, 2015.

Address correspondence to Susan W. Volk, V.M.D., Ph.D., University of Pennsylvania School of Veterinary Medicine, 312 Hill Pavilion, 380 S University Ave, Philadelphia, PA 19104-4539. E-mail: swvolk@vet.upenn.edu.

Breast cancer metastasis is the leading cause of cancer-related deaths in women worldwide. Collagen in the tumor microenvironment plays a crucial role in regulating tumor progression. We have shown that type III collagen (Col3), a component of tumor stroma, regulates myofibroblast differentiation and scar formation after cutaneous injury. During the course of these wound-healing studies, we noted that tumors developed at a higher frequency in $Col3^{+/-}$ mice compared to wild-type littermate controls. We, therefore, examined the effect of Col3 deficiency on tumor behavior, using the murine mammary carcinoma cell line 4T1. Notably, tumor volume and pulmonary metastatic burden after orthotopic injection of 4T1 cells were increased in $Col3^{+/-}$ mice compared to $Col3^{+/+}$ littermates. By using murine (4T1) and human (MDA-MB-231) breast cancer cells grown in Col3-poor and Col3-enriched microenvironments *in vitro*, we found that several major events of the metastatic process were suppressed by Col3, including adhesion, invasion, and migration. In addition, Col3 deficiency increased proliferation and decreased apoptosis of 4T1 cells both *in vitro* and in primary tumors *in vivo*. Mechanistically, Col3 suppresses the procarcinogenic microenvironment by regulating stromal organization, including density and alignment of fibrillar collagen and myofibroblasts. We propose that Col3 plays an important role in the tumor microenvironment by suppressing metastasis-promoting characteristics of the tumor-associated stroma. *(Am J Pathol 2015, 185: 1471–1486; http://dx.doi.org/10.1016/j.ajpath.2015.01.029)*

Breast cancer is the most frequently diagnosed cancer in women and is the leading cause of cancer-related deaths in women worldwide (World Health Organization: Latest World Cancer Statistics. 2013, Press Release Number 223, *http://www.iarc.fr/en/media-centre/pr/2013/pdfs/pr223_E.pdf*). In fact, >500,000 women are predicted to die this year alone. Without major changes in prevention or treatment, those numbers are anticipated to nearly double in 20 years. In most patients, death is not caused by the primary tumor, but rather by metastases. The extracellular matrix (ECM) of the tumor microenvironment plays a critical role in cancer development and progression through its ability to modulate physical, biochemical, and biomechanical cues perceived by both tumor cells and cancer-associated stromal cells.[1–3] Given this critical role of the ECM and tumor stromal cells in breast cancer development and progression, it is not surprising that recent studies suggest that targeting the tumor stroma is a potential therapeutic strategy for tumor control.[4–6] However, optimization of such strategies requires a better understanding of the mechanistic role that individual stromal components play in regulating tumor cell behavior.

Supported by National Institute of Arthritis and Musculoskeletal and Skin Diseases grant K08AR053945, the Mari Lowe Center for Comparative Oncology at the University of Pennsylvania School of Veterinary Medicine, a Jack Miller-Ebrahimi Foundation gift (S.W.V.), and NIH grants DK058123 (R.G.W.), R01CA180070, and RO1CA141144 (E.P.), and S10RR027128 (which funded Bruce D. Freedman for instrumentation in the Penn Vet Imaging Core facility).

Disclosures: None declared.

http://dx.doi.org/10.1016/j.ajpath.2015.01.029

Collagen, a major component of the ECM, is increasingly recognized to play a key role in regulating breast cancer progression. Although most research on collagen in breast cancer has focused on type I collagen (Col1), and many reports have documented a negative correlation between Col1 expression and prognosis in breast cancer patients, collagen types IV, V, VI, and XVIII have also been implicated in modulation of breast cancer cell activities and fate.[7–12] Increased collagen density in the tumor stroma can promote invasion and metastasis of breast cancer cells.[4,13–15] In addition, differences in the organization and stiffness of the tumor stroma are known to influence tumor cell responses and stromal remodeling, a key step in metastasis.[15–24] In fact, targeting collagen in the tumor stroma can effectively reduce pulmonary metastasis in breast cancer models.[4,6]

In contrast to the documented procarcinogenic effects of Col1, a gap in knowledge exists regarding the role for the related fibrillar type III collagen (Col3) in breast cancer. Col3 plays a critical function in tissue and organ maintenance, in part through its ability to regulate Col1 fibrillogenesis.[25] We have identified a role for Col3, distinct from Col1, in promoting a regenerative wound-healing response after cutaneous injury. Specifically, we showed that Col3 promotes reepithelialization and suppresses scar formation through its ability to limit the density of myofibroblasts, the key cellular effectors of scar formation/fibrosis, within wound granulation tissue.[26] Given the long-standing view of cancer as wounds that do not heal and the more recently described wound healing, chronic fibrosis, and cancer progression triad,[27,28] we hypothesized that diminished Col3 in the tumor microenvironment would drive aggressive cancer behaviors and promote metastasis. Because many of the same cells and extracellular proteins (eg, collagens and growth factors) that cause wound healing to go awry also drive aggressive cancer behavior,[27,28] it is noteworthy that myofibroblasts and a fibrotic healing response characteristic of Col3-deficient wounds have both been implicated in breast cancer metastasis.[29–31] Consistent with our hypothesis that Col3 loss promotes aggressive breast cancer behaviors, recent data show that a robust stromal response that includes increased Col3 expression correlates with improved survival of breast cancer patients.[32]

Herein, we present *in vitro* and *in vivo* evidence that Col3 plays an important role in suppressing breast cancer growth and metastasis, using murine (4T1) and human (MDA-MB-231) metastatic triple-negative breast cancer cell lines, a cancer type with limited effective treatment options. Specifically, we show that Col3 is a critical regulator of tumor stroma organization and that diminished levels of Col3 promote tumor cell survival, proliferation, and key processes in metastasis (adhesion, invasion, and migration). Collectively, our findings show that Col3 suppresses procarcinogenic behavior of breast cancer cells to limit primary tumor growth and metastasis and suggest that a Col3-deficient tumor microenvironment promotes metastasis, in part, through the impact of Col3 on stromal organization.

Materials and Methods

Col3-Deficient Mice

Animal use and care were approved by the Institutional Animal Care and Use Committee of the University of Pennsylvania (Philadelphia) and followed guidelines set forth in the NIH *Guide for the Care and Use of Laboratory Animals*.[33] All mice for this study were generated in a colony established at the University of Pennsylvania from breeder pairs of *Col3a1* heterozygous ($Col3^{+/-}$) mice originally purchased from Jackson Laboratories (Bar Harbor, ME). These mice had been generated by homologous recombination by replacement of the promoter region and first exon of the Col3 gene with a 1.8-kb PGKneo cassette,[25] generating a global knockout. Animals were genotyped for Col3 by PCR analysis of DNA extracted from tail biopsy specimens and were microchipped for identification (Allflex FDX-B transponders; Allflex USA, Inc., Dallas, TX).[26,34]

All mice in the Col3 colony, regardless of the study they were used for, were surveyed routinely for general health and pathology, including gross evidence of tumor development. Once a trend was recognized for an increase in tumor formation in $Col3^{+/-}$ mice, all mice dying spontaneously or euthanized at >1 year of age had a gross necropsy performed, and a biopsy of any abnormal masses was performed. Histopathological diagnoses of tumor biopsy specimens were made by a board-certified veterinary pathologist (E.A.M.).

Cell Culture and Tumor Generation

4T1 and 4T1–green fluorescent protein (GFP) cell lines (obtained from Dr. Lalage Wakefield at the National Cancer Institute, Bethesda, MD, in 2010[35]) and MDA-MB-231 cells [obtained from Dr. Meenhard Herlyn (Wistar Institute, Philadelphia, PA) in 2012[36]] were authenticated by morphology, growth characteristics, and biological behavior, tested for *Mycoplasma*, and frozen. Cells were cultured for <4 months. All cells were cultured in growth media: Dulbecco's modified Eagle's medium (Glutamax; Gibco, Grand Island, NY) supplemented with 10% fetal bovine serum (Atlanta Biologicals, Flowery Branch, GA) and antibiotics (100 U/mL penicillin and 100 g/mL streptomycin). GFP expression in the 4T1-GFP cell line was preserved with inclusion of 50 μg/mL G418 (Geneticin, Life Technologies, Carlsbad, CA) in the growth media.

For orthotopic tumor implantation, 0.1 or 0.5×10^6 4T1 cells [in 0.1 mL sterile phosphate-buffered saline (PBS)] were injected s.c. into the right fourth mammary fat pad of anesthetized mice (aged 8 to 20 weeks). Tumor volume was calculated using the following formula: $V = (L \times W^2)/2$.[37]

Tissue Processing

Primary tumors, mammary fat pads, and lungs were collected and fixed in Prefer Fixative (Anatech LTD, Battle

Creek, MI). Before fixation, lungs were perfused through the heart and trachea. Tissues were paraffin embedded and processed, and serial sections (4 μm thick) were stained with hematoxylin and eosin (H&E), as previously described.[26]

Analysis of Pulmonary Metastases

After perfusion and fixation, gross lung metastases in mice with orthotopic 4T1 tumors were counted. All lung lobes were bisected lengthwise through the main stem bronchi.[38] Quantitation of metastasis on H&E-stained slides containing a cross section of all five lung lobes was performed by a pathologist (E.A.M.). Lung tumor burden was quantitated using ImageJ software version 1.48 (NIH, Bethesda, MD), as previously described.[39] To examine how Col3 in the metastatic niche regulates metastasis, tail vein injections and analysis of pulmonary colonization were performed. Specifically, 7- to 11-week-old male mice were injected with 1.0×10^6 4T1-GFP cells (via tail vein). After 24 hours, the mice were sacrificed, and the lungs were perfused with PBS. A single-cell suspension was collected after treating the lungs with a mixture of collagenases. Cells were stained with propidium iodine and analyzed via flow cytometry using a LSRFortessa (BD Biosciences, Bedford, MA). The percentage of live (propidium iodine−negative) 4T1 (GFP-positive) cells within the lung was calculated.

Tissue Immunohistochemistry and Immunofluorescence

Sections from fixed, paraffin-embedded tissues were mounted onto charged glass slides. After deparaffinization and rehydration, antigen retrieval was performed by citrate buffer boiling or incubation with proteinase K (20 μg/mL in Tris-ethylenediaminetetraacetic acid buffer for Col3 staining).

For immunohistochemistry, sections were blocked in 3% H_2O_2, PBS containing 1% bovine serum albumin (A5611; Sigma-Aldrich, St. Louis, MO), 10% goat serum, avidin blocking solution, and biotin blocking solution (Avidin Blocking Kit; Vector Laboratories Inc., Burlingame, CA). For immunofluorescence, sections were blocked in PBS containing 5% bovine serum albumin, 5% goat serum, and 0.05% Tween-20 (Bio-Rad, Hercules, CA). Slides were incubated with antibodies directed against Col3 (ab7778; Abcam, Cambridge, MA), Ki-67 (ab15580; Abcam), active caspase 3 (9664; Cell Signaling, Danvers, MA), or α-smooth muscle actin (α-SMA; ab5694; Abcam). Slides were then incubated in secondary antibody, biotin-goat anti-rabbit IgG (BA 1000; Vector Laboratories Inc.), then incubated in tertiary antibody (ABC elite; Vector Laboratories Inc.) and incubated in DAB+ Substrate (Dako, Carpinteria, CA) until brown color developed. Slides were counterstained in hematoxylin, before dehydration and mounting.

For immunofluorescence, sections were incubated with an Alexa Fluor 488 goat anti-rabbit antibody (Invitrogen, Grand Island, NY) and mounted in medium containing DAPI (Vector Laboratories Inc.). All slides were viewed with an Olympus BX51 microscope (Olympus, Melville, NY), and digital images were obtained using a constant exposure threshold. For active caspase 3 and α-SMA staining quantification, ImageJ software was used to measure the percentage area of the image that contained positive staining. The proliferative index was calculated using ImageJ software (percentage of Ki-67−positive nuclei/total nuclei).

Quantitative Real-Time PCR

mRNA expression analysis was performed as previously described.[34] Briefly, RNA was extracted from fibroblasts, 4T1 cells, and mouse tissues [mammary fat pads and lungs from tumor-naïve mice and tumors (14 days after orthotopic injection of 4T1 cells)], cDNA was generated, and Col1 and Col3 expression was compared to glyceraldehyde-3-phosphate dehydrogenase as the endogenous control. For mouse tissues, lungs from young (16 to 18 weeks old) and aged (92 to 94 weeks old), and fat pads and tumors from young (10 to 24 weeks old), mice were used.

Fibroblast Isolation and Culture

Embryonic fibroblasts were harvested and genotyped as described previously.[26] Fibroblasts were cultured and passaged (passage 6 or less), as described for 4T1 cells, including the addition of L-ascorbic acid (A8960; Sigma-Aldrich) to the growth media to ensure secretion of a collagen-rich matrix.

Generation of Fibroblast-Derived Matrices

Decellularized matrices were generated, as previously described,[40] using E18.5 embryonic fibroblasts. After 5 to 8 days in culture, the matrices were decellularized and were either stored in PBS at 4°C or used immediately for experiments.

Proliferation Assays

Fibroblast-derived matrices were generated in 96-well plates (1.0×10^4 fibroblasts per well), as described above. 4T1 (1.5×10^4) or MDA-MB-231 (2.5×10^4) cells were plated and cultured on these decellularized matrices in growth media for 6 hours before changing to serum-free media overnight. Proliferation was measured using a bromodeoxyuridine, 96-well, enzyme-linked immunosorbent assay−based assay (QIA58; EMD Millipore, Billerica, MA), using a Varioskan Flash plate reader (Thermo Fisher Scientific, Waltham, MA).

Analysis of Apoptotic Cells

4T1 or MDA-MB-231 cells (1.0×10^4) were plated onto fibroblast-derived matrix-coated coverslips in 24-well plates, cultured in growth media for 16 hours, and then switched to serum-free media for 48 hours. After fixation with 4% paraformaldehyde, coverslips were incubated with an

antibody directed against active caspase 3 (ab2302; Abcam) and subsequently with an Alexa Fluor 488 donkey anti-rabbit antibody (Invitrogen), before mounting in medium containing DAPI. Fluorescence was viewed as described above for sections.

Adhesion Assays

For assessment of Col3 modulation of 4T1 morphology and adhesion, fibroblasts (5.0×10^4) were plated and cultured in 24-well plates for 48 hours in growth media before subsequent seeding of 4T1-GFP cells (8.0×10^5). 4T1-GFP cells were allowed to adhere for 2 hours in growth media or remain in culture for 48 hours in serum-free media to assess morphology, then fixed and imaged. For adhesion, GFP intensity was quantitated using ImageJ software. For adhesion in collagen-coated wells, 24-well plates were coated with 0.5 μg/cm^2 human placenta-derived (hP) collagens hPCol1 (354243; BD Biosciences), hPCol3 (354244; BD Biosciences), or a 50:50 (0.5 μg/cm^2 total collagen) or 100:50 (0.75 μg/cm^2 total collagen) mixture of both. 4T1 cells (5.0×10^5) were plated in growth media and allowed to adhere for 2 hours. Attached cells were stained with crystal violet, and OD 570 was measured using a Varioskan plate reader. For adhesion to a substratum with stiffness similar to mammary fat pad,[41] hydrogels (6 kPa) were generated as described previously[42] on 12-mm coverslips in 24-well plates. The hydrogels were coated with hPCol1 and hPCol3 at 0.03 mg/mL or a 50:50 mixture of both. 4T1-GFP cells were allowed to attach as described above, and GFP intensity (509 nm) was read in a Varioskan plate reader. Data between separate experiments were normalized to gels coated with rat tail collagen (354236; BD Biosciences). For MDA-MB-231 adhesion in collagen-coated wells, MDA-MB-231 cells (2.5×10^5) were plated in growth media and allowed to adhere for 1 hour, and analyzed as above for 4T1 cells.

Invasion and Migration Assays

Migration was assessed in 24-well Transwell plates (353097; BD Biosciences) that were coated with 1 μg/cm^2 recombinant human Col1 (354254; BD Biosciences), recombinant human Col3 (354255; BD Biosciences), or a 50:50 mixture of both. 4T1 or MDA-MB-231 cells (5.0×10^5) were plated in the upper chambers in serum-free media and allowed to migrate for 20 hours (lower chamber contained growth media). Cells collected from the bottom of the porous membrane were stained with crystal violet, which was quantitated as above. Invasion was assessed similarly, except that the collagens were added to Matrigel (354230; BD Biosciences) used to coat the top of the membranes before cell seeding. Cancer cells that invaded through the collagen-supplemented simulated basement membrane were quantitated as described above. For MDA-MB-231 invasion and migration, hPCol1, hPCol3, or a 50:50 mixture of both was used.

Second Harmonic Generation and Collagen Fiber Analysis

Imaging of fibrillar collagen was performed on a Leica SP5 confocal/multiphoton microscope (Leica Microsystems, Inc., Mannheim, Germany) by tuning the Coherent Chameleon Ultra II Ti:Sapphire laser (Coherent Inc., Santa Clara, CA) to 800 nm and collecting second harmonic (SHG) signal on a non-descanned detector configured to capture wavelengths <495 nm. To distinguish true SHG signal from autofluorescence, fluorescence images at wavelengths of 495 to 560 nm (green autofluorescence) and 560 to 620 nm (red autofluorescence) were simultaneously acquired on two additional nondescanned detectors and subtracted from the original SHG image. Collagen signal and orientation were analyzed as described previously,[43] with few modifications. ImageJ software was used to calculate the percentage of the images that contained SHG-positive pixels, as a measure of collagen fiber intensity. ImageJ software was then used to generate a fast Fourier transform powerplot of the fibrillar collagen signal. An ellipse was superimposed over the positive signal, and the major and minor axes of the ellipse were measured. An aspect ratio (major/minor axis) with a smaller value indicated random orientation, and larger values indicated orientated, aligned collagen fibers. For quantification of tumor-associated collagen signature (TACS), fibers at the tumor boundary were analyzed using CurvAlign software (*http://loci.wisc.edu/software/curvealign*, last accessed December 31, 2014; version 3.0, beta 2). The sum of all collagen fibers with angles between 0 and 30 degrees from the tumor boundary was considered to be TACS-2, and fibers with angles between 60 and 90 degrees were classified as TACS-3, as previously described.[44]

Data Analysis

Values are expressed as means ± SD, unless otherwise stated. A one-tailed Fisher's exact test was performed to compare spontaneous tumor incidence between Col3$^{+/+}$ and Col3$^{+/-}$ mice. For *in vivo* experiments, unpaired Student's *t*-tests were used to determine the significance of differences between mouse genotypes. For *in vitro* analyses, paired *t*-tests were used to compare fibroblasts from littermate embryos that were isolated, cultured, frozen, and passaged together. One-way analyses of variance, followed by Tukey post hoc tests, were used to compare cancer cell properties on different collagens. Study groups were compared using GraphPad Prism 5 statistical software (La Jolla, CA). $P < 0.05$ was considered statistically significant.

Results

Col3 Haploinsufficiency Promotes Development of Spontaneous Neoplasia

During our original wound-healing studies,[26] we noted that spontaneous tumors developed more frequently in aged (>1

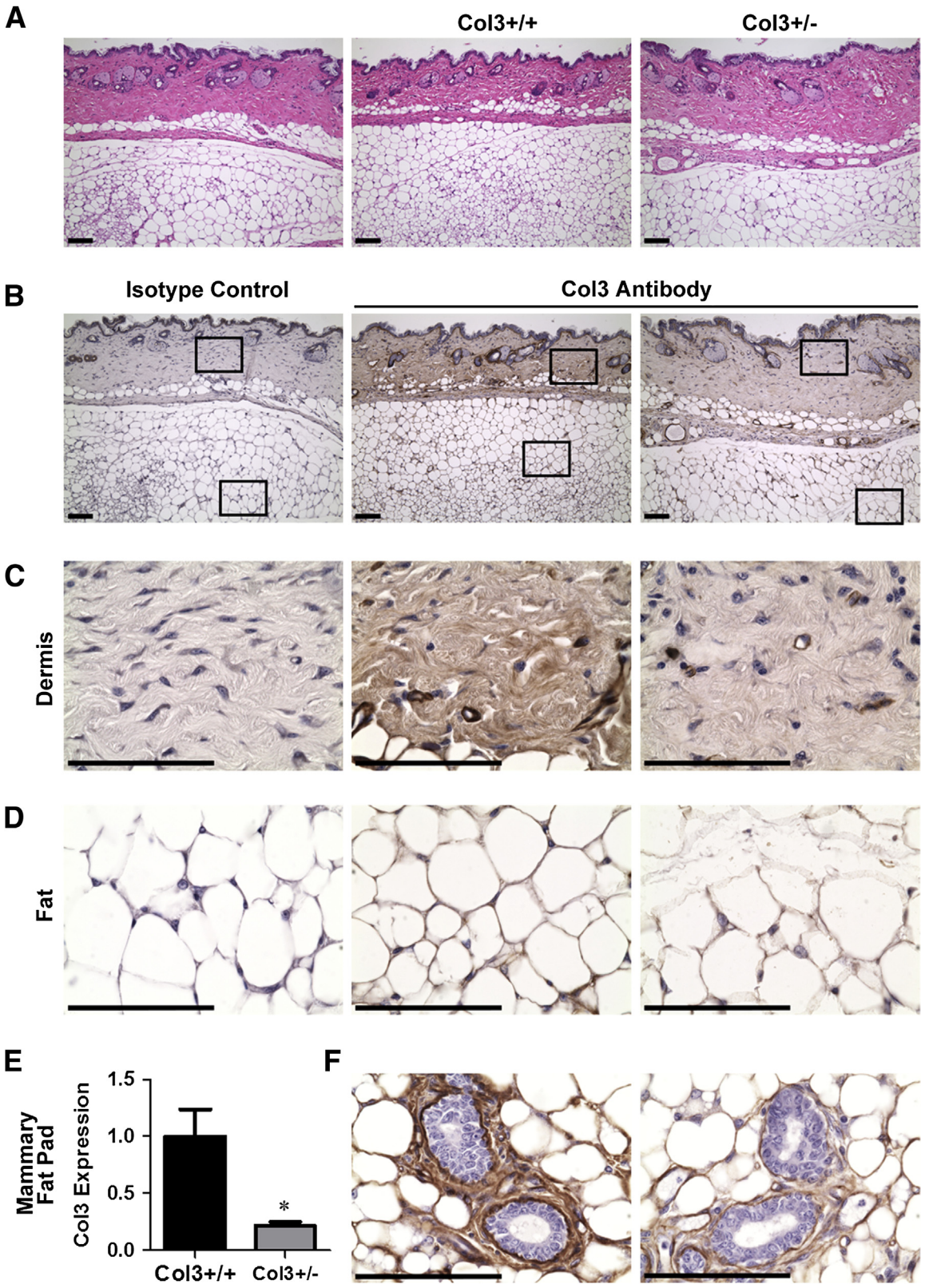

Figure 1 Expression of $Col3^{+/-}$ is reduced in fat pads from Col3 mice compared to wild-type ($Col3^{+/+}$) mice. **A:** Images of skin and adjoining s.c. fat from fat pads stained with hematoxylin and eosin. **B:** Serial sections from **A** stained for Col3. **Left panel:** Isotype control. **Middle panel:** Col3-stained $Col3^{+/+}$ tissue sections. **Right panel:** Col3-stained $Col3^{+/-}$ tissue sections. **Boxed areas** are enlarged in **C** and **D**. **C:** Images of Col3-stained dermis. **D:** Images of Col3-stained fat. **E:** mRNA expression of Col3 from mammary fat pads relative to $Col3^{+/+}$ fat pads. **F:** Images of Col3-stained mammary glands within the mammary fat pad. Representative images shown (**A**–**D** and **F**). Data represent means ± SEM (**E**). $n = 4$ $Col3^{+/+}$ and $Col3^{+/-}$ (**E**). $^*P < 0.05$ (**E**). Scale bars: 100 μm. Original magnifications: ×10 (**A**); ×60 (**C**, **D**, and **F**).

year) female Col3$^{+/-}$ mice compared to age- and sex-matched wild-type littermates [12/73 (16.4%) Col3$^{+/-}$ mice versus 3/58 (5.2%) Col3$^{+/+}$ mice; $P < 0.05$]. Histopathology confirmed the diagnosis of neoplasia in all masses on which a biopsy was performed (13 masses total) (Supplemental Table S1). Although a variety of tumor types were represented, mammary carcinoma was found in two Col3$^{+/-}$ mice (Supplemental Figure S1). Given the increased incidence of spontaneous tumor development in Col3$^{+/-}$ mice and the potential role of Col3 in suppressing aggressive breast cancer behavior in women,[32] we initiated a study to examine mammary tumor growth and metastasis in Col3-deficient mice, using the syngeneic 4T1 model of breast cancer.[35,45]

Col3 Haploinsufficiency Promotes Primary Tumor Growth and Metastasis

Liu et al[25] previously generated Col3$^{-/-}$ mice by homologous recombination, replacing the promoter and the first exon of the *Col3a1* gene with a neomycin cassette. Because these global knockout mice rarely survive beyond the perinatal period,[25] we used Col3-haploinsufficient mice, which have been confirmed to express ≤50% Col3 in all tissues examined,[25,34,46,47] to study the effects of Col3 on mammary tumor development. Fibrillar collagens, including Col3, are ECM components of normal human and rodent mammary tissue.[48,49] Immunohistochemical localization of Col3 within the skin and underlying s.c. fat, including mammary tissue, in Col3$^{+/+}$ mice revealed Col3 staining surrounding blood vessels and within the dermis, periadipocyte matrix, and the intralobular stroma of mammary ducts (Figure 1). By comparison, Col3 immunostaining appeared less pronounced in sections from tissues harvested from Col3$^{+/-}$ mice. Quantitative real-time PCR confirmed a significant reduction in Col3 expression in the mammary fat pad of young adult Col3$^{+/-}$ mice compared to wild-type littermates ($P < 0.05$).

To determine whether diminished levels of Col3 drive aggressive tumor behaviors, 4T1 cells were injected orthotopically in Col3 wild-type and haploinsufficient littermates, and primary tumor growth and metastasis were assessed. Primary tumor size was measured every 2 to 3 days after injection of 4T1 cells into either Col3$^{+/+}$ or Col3$^{+/-}$ mice. By day 21, primary tumors in Col3$^{+/-}$ mice were twice as large as tumors in Col3$^{+/+}$ mice (Figure 2A). Both the cumulative effect of Col3 deficiency on 4T1 tumor growth, analyzed by measuring the area under the curve for each tumor[50] and the tumor mass at the study end point (day 24) (Figure 2, B and C), confirmed that tumor growth is significantly increased by Col3 deficiency.

Because mortality in breast cancer patients is almost always associated with metastases rather than the primary tumor, we investigated whether Col3 deficiency also increased pulmonary metastasis in the 4T1 breast cancer model (Figure 2, D–H). Quantitative analysis revealed a nearly threefold increase in gross metastases in Col3$^{+/-}$ compared to Col3$^{+/+}$ lungs ($P < 0.05$) (Figure 2F). Quantitative histological assessment of H&E-stained lung sections confirmed that both the number of metastatic nodules and the tumor burden (% total lung area) were significantly greater in Col3$^{+/-}$ mice compared to Col3$^{+/+}$ littermates (Figure 2, G and H).

We next investigated whether diminished Col3 in the pre-metastatic niche (lung) of Col3$^{+/-}$ mice increased pulmonary parenchymal colonization of metastasized cells. Collagen, including Col3, is a normal component of the lung, with Col3 expression attributed to pulmonary fibroblasts in several studies.[51–53] As anticipated in this global knockout Col3 strain, pulmonary Col3 was significantly reduced in Col3$^{+/-}$ mice compared to Col3$^{+/+}$ littermates (Figure 3A). As suggested by previous studies examining the effect of age on Col3 expression,[34,54–57] advanced age (>23 months) is associated with a reduction in pulmonary Col3 mRNA expression ($P < 0.01$). To assess whether reduced pulmonary Col3 could influence tumor colonization of the lungs, 4T1-GFP cells were injected via the tail vein into young adult Col3$^{+/+}$ and Col3$^{+/-}$ mice. After 24 hours, the percentage of GFP-positive live cells in single lung cell suspensions was quantitated by flow cytometry (Figure 3, B and C). There was no significant difference between cells colonizing lungs of Col3$^{+/+}$ and Col3$^{+/-}$ mice, suggesting that Col3 limits pulmonary metastasis primarily through another mechanism, such as a gatekeeper effect at the level of the primary tumor site. Taken together, our results identify a previously unrecognized role for Col3 as a suppressor of breast cancer growth and metastasis and distinguish the effects of Col3 from the procarcinogenic effects of Col1 in the tumor microenvironment.

Col3 Deficiency Promotes Proliferation and Inhibits Apoptosis of Breast Cancer Cells

An increase in proliferation, a decrease in apoptosis, or both could mediate the accelerated primary tumor growth seen in Col3$^{+/-}$ mice. To differentiate between these possibilities, we examined bromodeoxyuridine incorporation and active caspase 3 activity in 4T1 cells cultured on wild-type and Col3-deficient cell-derived matrices *in vitro*. Col3-deficient decellularized matrices were prepared from Col3$^{-/-}$ embryonic fibroblasts, because culture and passage could potentially induce variations in Col3 production by Col3$^{+/-}$ fibroblasts. Increased bromodeoxyuridine incorporation was observed in 4T1 cells cultured on Col3$^{-/-}$ fibroblast-derived matrices, relative to that seen with cells cultured on Col3$^{+/+}$ fibroblast-derived matrices ($P < 0.05$) (Figure 4A). In addition, there was a significant decrease in active caspase 3 staining in 4T1 cells cultured on matrices lacking Col3 (Col3$^{-/-}$) after serum deprivation (Figure 4B). Similar trends for proliferation and apoptosis were also seen in human MDA-MB-231 breast cancer cells cultured on Col3-deficient matrices relative to wild-type matrices (Supplemental Figure S2, A and B). Consistent with these *in vitro* findings, tumor cell proliferation was significantly increased and apoptosis was significantly decreased in 4T1 tumors grown in Col3$^{+/-}$ mice compared to Col3$^{+/+}$ littermates, as evidenced

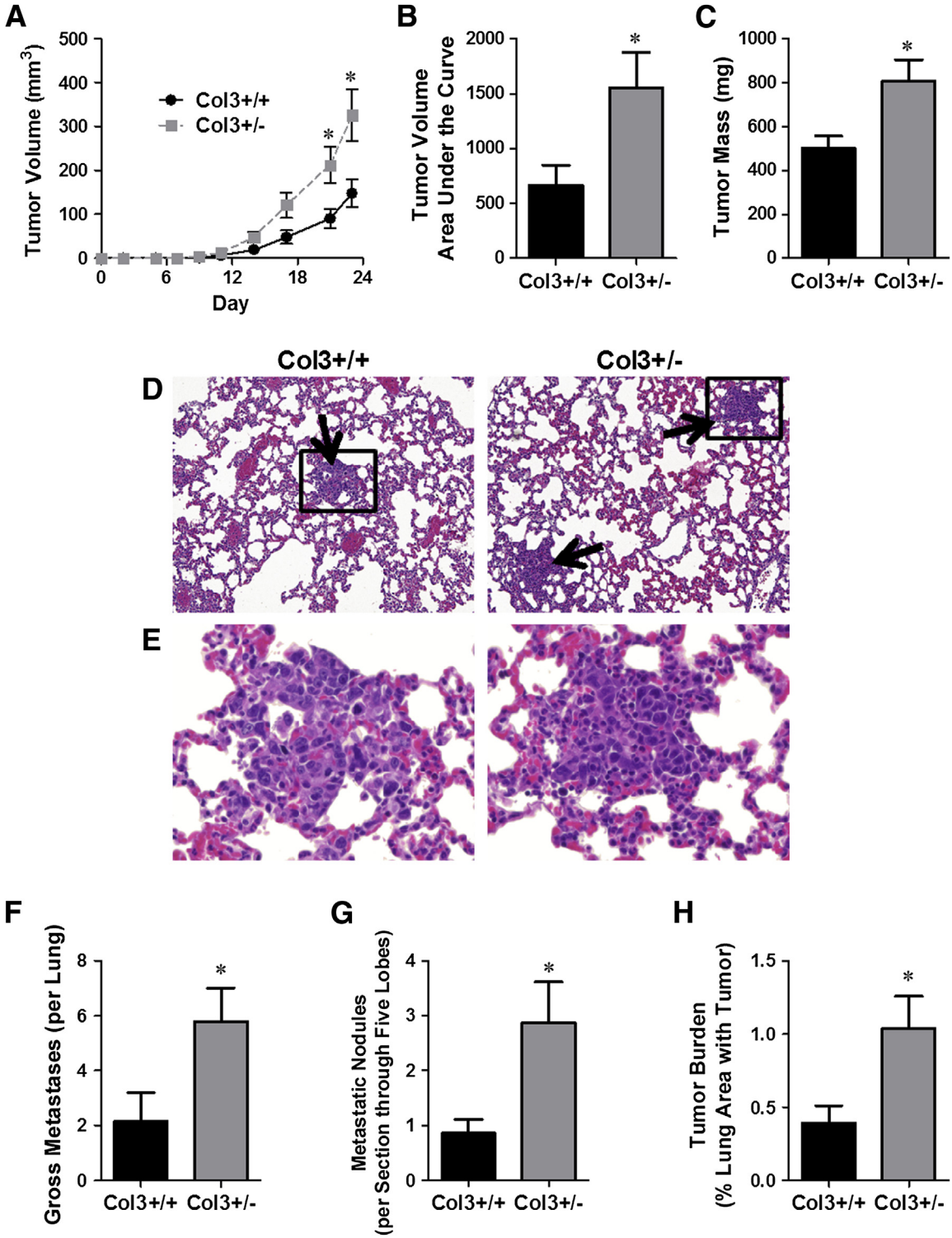

Figure 2 Orthotopic murine (4T1) mammary tumor growth and metastasis to the lung are limited by type III collagen (Col3). **A:** Tumor growth was measured in 4T1 tumor-bearing (0.1×10^6 cells injected) female $Col3^{+/+}$ and $Col3^{+/-}$ mice using calipers. **B:** To compare the cumulative pattern of tumor growth, the area under the curve was calculated for each tumor. **C:** The mass of the tumors was determined at the time of sacrifice (day 24). **D** and **E:** Hematoxylin and eosin (H&E) sections of lungs from $Col3^{+/+}$ and $Col3^{+/-}$ mice bearing orthotopic 4T1 tumors. **Arrows** point to metastatic nodules. **Inset** is magnified in **E**. **F:** Gross metastases were counted on lung lobe surfaces. **G:** The number of metastatic nodules within H&E-stained sections of all five bisected lung lobes of 4T1-bearing $Col3^{+/+}$ and $Col3^{+/-}$ mice, as assessed by a board-certified pathologist (E.A.M.). **H:** Lung metastatic tumor burden (tumor area over total lung area) was calculated from the same images in **G** using ImageJ software. Representative data from five independent experiments with the injection of 0.1 to 5.0×10^6 cells all show increased metastases in $Col3^{+/-}$ animals (quantitative data shown after orthotopic injection of 0.1×10^6 4T1 cells). Data represent means ± SEM (**A**–**C** and **F**–**H**). $n = 7$ to 10 mice per genotype (**A**–**C** and **F**–**H**). *$P < 0.05$ (**A**–**C** and **F**–**H**).

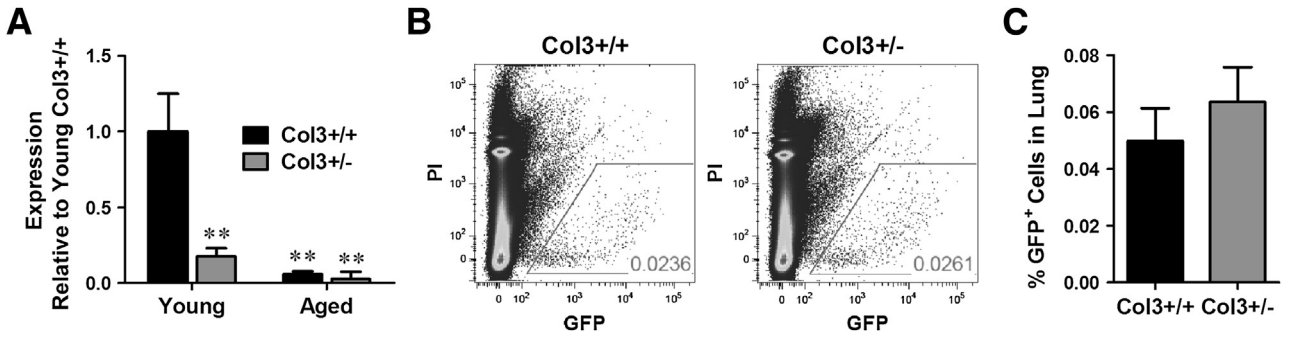

Figure 3 Type III collagen (Col3) does not affect initial murine (4T1)—green fluorescent protein (GFP) cell adhesion and colonization in the lung. **A:** Col3 mRNA expression in lungs from young and aged mice relative to young $Col3^{+/+}$ lungs. **B** and **C:** 1.0×10^6 4T1-GFP cells were injected via the tail vein into young adult $Col3^{+/+}$ and $Col3^{+/-}$ mice. After 24 hours, lungs were harvested and processed into single-cell suspensions. The percentage live [propidium iodine (PI)—negative] 4T1 cells (GFP positive) within the lung was quantified by flow cytometry. Data represent means ± SEM (**A** and **C**). $n = 4$ $Col3^{+/+}$ and $n = 6$ $Col3^{+/-}$ (**A**, young mice); $n = 3$ $Col3^{+/+}$ and $n = 3$ $Col3^{+/-}$ (**A**, aged mice); $n = 10$ to 12 per genotype (**C**). $^{**}P < 0.01$.

by Ki-67 and active caspase 3 staining, respectively (Figure 4, C–F). Thus, both mechanisms (increased proliferation and decreased apoptosis) contribute to increased primary tumor growth in $Col3^{+/-}$ mice compared to wild-type littermates.

Col3 Deficiency Promotes a Metastatic Phenotype *in Vitro*

To mimic the effects of the tumor stroma in an *in vitro* system, we co-cultured 4T1 cells with wild-type ($Col3^{+/+}$) and $Col3^{-/-}$ mouse embryonic fibroblasts. We observed a marked increase in 4T1 cell numbers in the presence of $Col3^{-/-}$ fibroblasts (Figure 5A). We also observed a striking difference in 4T1 cell morphology (Figure 5A). Consistent with cell morphology on tissue culture plastic, 4T1-GFP cells co-cultured with wild-type ($Col3^{+/+}$) fibroblasts grew as aggregates. In contrast, when co-cultured with $Col3^{-/-}$ fibroblasts, cells dispersed throughout the culture (Figure 5A). Adhesion assays demonstrated that the number of adherent 4T1 cells was significantly increased when plated onto $Col3^{-/-}$ fibroblasts compared to $Col3^{+/+}$ fibroblasts (Figure 5, B and C), suggesting that this dispersed phenotype may, at least in part, be due to Col3-dependent alterations in cell adhesion. To determine whether Col3 directly affects adhesion or whether this effect is instead mediated by modulation of fibroblast phenotype, we plated 4T1 cells in wells coated with Col3, mixtures of Col1/3, or Col1. Even in the absence of fibroblasts, 4T1 adhesion was decreased on a Col3 substrate compared to Col1 substrate alone (Figure 5D). Adhesion of 4T1 cells on a mixture of the two collagens (50:50, total collagen constant) was intermediate between either collagen alone. To ensure that the decreased adhesion of 4T1 cells was due to an increase in Col3 rather than loss of Col1, we also examined 4T1 adhesion on a collagen substrate of constant Col1 and additional Col3 (Col1/3, 100:50). Even with an increase in total collagen, the addition of Col3 significantly reduced 4T1 adhesion. Col3-induced changes in cell spreading, attachment strength, and survival may have also contributed to these findings given the 2-hour time points used in this set of assays.

Because the stiffness of the tumor microenvironment can affect cell adhesion,[58] we also compared adhesion of 4T1 cells to the fibrillar collagens (Col1, Col3, or Col1/3, 50:50 mixture) on hydrogels of physiologically relevant stiffness (6 kPa),[41] which are significantly softer than tissue culture plastic. 4T1 cell adhesion to Col3-, Col1/3-, and Col1-coated hydrogels again confirmed that Col3 significantly reduced the number of attached 4T1 cells (Supplemental Figure S3). Thus, on a matrix of biologically relevant stiffness, Col3 directly reduces breast cancer adhesion. Adhesion of human MDA-MB-231 cells was also significantly decreased on Col3 compared to Col1 (Supplemental Figure S2C), thus supporting a shared response to Col3 by triple-negative breast cancer cells in mice and humans.

Given the increased incidence of metastasis associated with Col3 haploinsufficiency in the 4T1 model of murine breast cancer, we examined the ability of Col3 to modulate invasion and migration of breast cancer cells through basement membrane gels supplemented with Col3, a 50:50 mixture of Col1 and Col3, or Col1 alone using standard *in vitro* Transwell assays.[59] Invasion of 4T1 or MDA-MB-231 cells was significantly inhibited in Col3-containing gels compared to gels with Col1 alone (Figure 6, A and C, and Supplemental Figure S2D). Similarly, the presence of Col3 resulted in a significant reduction in 4T1 and MDA-MB-231 cell migration (Figure 6, B and D, and Supplemental Figure S2E). Thus, Col3 directly limits murine and human breast cancer cell invasion and migration, supporting the hypothesis that Col3 suppresses metastatic escape at the level of the primary tumor.

Col3 Deficiency Promotes a Procarcinogenic Stroma by Regulating Collagen and Myofibroblast Density and Alignment

Collagen reorganization is increasingly recognized as a key determinant of a procarcinogenic microenvironment, with increasing collagen alignment facilitating metastasis.[16,18,21,24] Compared to a complex or disorganized matrix, aligned collagen provides a directed pathway for tumor cells to migrate

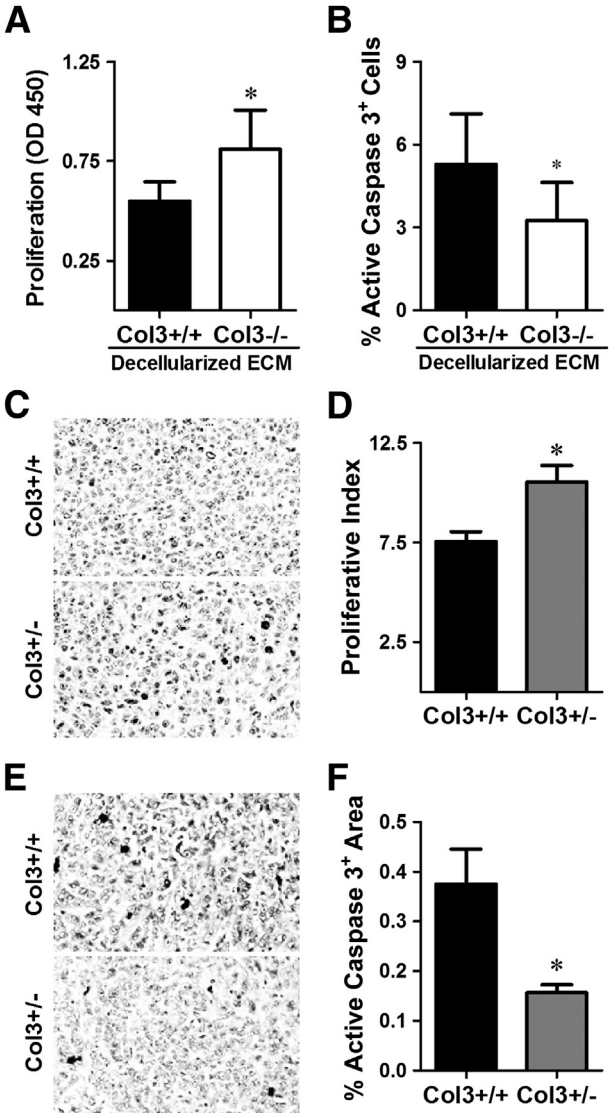

Figure 4 A type III collagen (Col3)—deficient microenvironment promotes breast cancer cell proliferation and inhibits cell death. **A:** Proliferation of murine (4T1) cells on Col3-rich and Col3-null native fibroblast-derived matrices was analyzed using a bromodeoxyuridine cell proliferation assay. Four different littermate embryonic fibroblast pairs ($Col3^{+/+}$ and $Col3^{-/-}$) were used to generate matrices. **B:** Apoptosis of 4T1 cells grown on $Col3^{+/+}$ and $Col3^{-/-}$ matrices after 48-hour serum starvation was analyzed by immunofluorescence staining for active caspase 3. Three littermate embryonic fibroblast pairs ($Col3^{+/+}$ and $Col3^{-/-}$) were examined in triplicate (five images per well). **C:** Tumor sections from $Col3^{+/+}$ and $Col3^{+/-}$ mice were stained for Ki-67 as a marker of proliferating cells. **D:** Proliferative index (percentage Ki-67—positive nuclei) was calculated. **E:** Tumor sections from $Col3^{+/+}$ and $Col3^{+/-}$ mice were stained for active caspase 3 as a marker of apoptosis. **F:** Active caspase 3 signal (active caspase 3—positive area) was calculated. For both proliferation and apoptosis staining in tumors, five random images that did not contain tumor edge or necrotic regions were taken per tumor. Data represent means ± SEM (**D** and **F**). $n = 7$ tumors per genotype (**D** and **F**). *$P < 0.05$. Original magnification, ×20 (**C** and **E**). ECM, extracellular matrix.

on and invade surrounding tissues. To determine whether Col3 potentially regulates fibrillar collagen production and organization in the tumor stroma, we performed collagen SHG imaging of fibroblast-derived matrices (Figure 7A) and found that $Col3^{-/-}$ fibroblasts produced a more highly aligned and fibrillar matrix than wild-type cells (Figure 7, B—D). To confirm that Col3 regulates stromal organization of breast cancer *in vivo*, 4T1 tumors were harvested from mice after 14 days. The H&E-stained tumor sections showed no obvious differences in general tumor morphology between genotypes (Figure 7E). However, when sections were imaged using SHG (Figure 7F), the tumors from Col3-deficient ($Col3^{+/-}$) mice contained more mature and aligned collagen fibers than the tumors from $Col3^{+/+}$ mice, similar to that seen with the fibroblast-derived matrices. Furthermore, at the tumor periphery, collagen fibers exhibited a more invasive phenotype characterized by alignment perpendicular to the tumor border in $Col3^{+/-}$ mice compared to that seen in $Col3^{+/+}$ mice (Supplemental Figure S4). Stromal collagen density and organization at the tumor boundary can be characterized using SHG to generate TACS scores. The invasive TACS-3 has been shown to correlate with aggressive behavior in murine breast cancer models[15,18,44] and has been established as an independent prognostic indicator in women regardless of tumor subtype, grade, and size, hormone receptor status, and lymph node status.[16,19,24] TACS analysis confirmed a significant decrease in the noninvasive TACS-2 signature ($P < 0.01$) and a significant increase in the invasive TACS-3 signature ($P < 0.05$) in tumors of Col3-haploinsufficient mice compared to wild-type littermates (Supplemental Figure S4).

Given our previous finding that Col3 deficiency drives myofibroblast differentiation and scar formation after cutaneous injury,[26] we next investigated whether $Col3^{+/-}$ tumors contained more myofibroblasts than tumors in $Col3^{+/+}$ mice. On the basis of expression of α-SMA, a marker of myofibroblasts (Figure 7, G and H), we found that tumors in $Col3^{+/-}$ mice had significantly increased stromal myofibroblast density. CD31 immunofluorescence confirmed that most α-SMA—positive cells were not associated with vascular smooth muscle cells (data not shown). In addition, $\alpha\text{-SMA}^{+}$ cells were organized in a striking, highly aligned pattern in the tumors of $Col3^{+/-}$ compared to $Col3^{+/+}$ mice (Figure 7I), suggesting that Col3 directs matrix organization or the ability of fibroblasts to interact with that matrix.

To determine Col3 expression and localization within the stroma, we performed immunohistochemistry for Col3 in tumors (14 days after orthotopic injection). Although there was marked heterogeneity in the density of Col3 throughout the tumors of both $Col3^{+/+}$ and $Col3^{+/-}$ mice (Figure 8), Col3 was found to be more aligned within tumors of Col3-haploinsufficient mice compared to wild-type littermates, similar to overall fibrillar collagen and myofibroblast organization. Because multiple studies have shown that tumor cells can contribute to stromal collagen production, we investigated whether 4T1 cells produce Col1, Col3, or both. Compared to $Col3^{+/+}$ fibroblasts, neither Col3 nor Col1 expression could be detected in cultured 4T1 cells, even when cultured on decellularized fibroblast matrices from either $Col3^{+/+}$ or $Col^{-/-}$ fibroblasts (Supplemental Figure S5). This is consistent with a previous study showing that stromal Col3

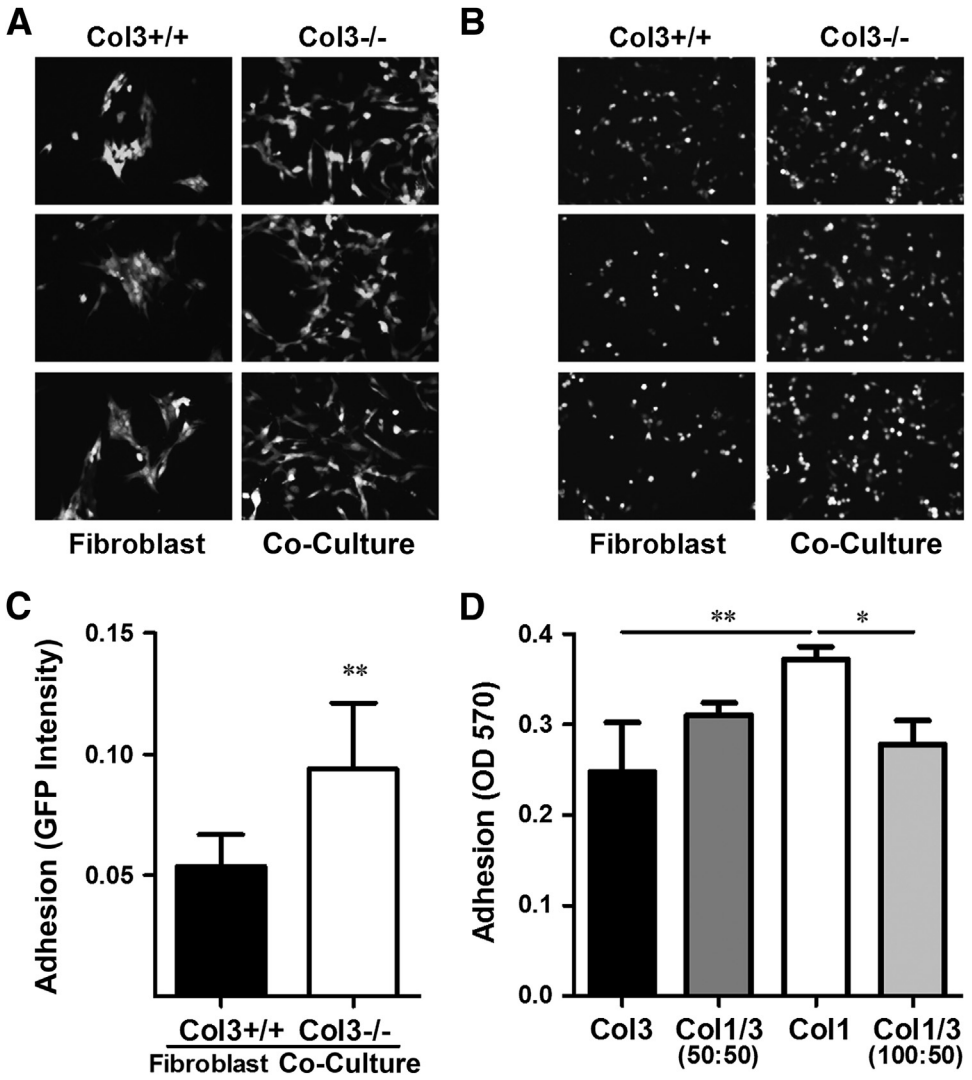

Figure 5 Murine (4T1) tumor cell morphology is changed and adhesion is enhanced in type III collagen (Col3)—null microenvironments. **A:** Morphology of 4T1—green fluorescent protein (GFP) cells co-cultured with $Col3^{+/+}$ and $Col3^{-/-}$ fibroblasts in serum-free media for 48 hours. Four different littermate embryonic fibroblast pairs were analyzed (three representative pairs shown). **B:** Images of 4T1-GFP cells after 2 hours in co-culture with $Col3^{+/+}$ and $Col3^{-/-}$ fibroblasts. **C:** Quantitative analysis of five different littermate embryonic fibroblast pairs (three representative pairs shown in **B**), evaluated in triplicate culture wells (five images per well). **D:** 4T1-GFP cells were allowed to attach for 2 hours to tissue culture plastic wells coated with the following: 0.5 $\mu g/cm^2$ Col3; a 50:50 mixture of Col1 and Col3 (Col1/3, 50:50; total collagen = 0.5 $\mu g/cm^2$); 0.5 $\mu g/cm^2$ Col1; or a 100:50 mixture of Col1 and Col3 (Col1/3, 100:50; total collagen = 0.75 $\mu g/cm^2$). Attached cells were fixed and stained with crystal violet and read at OD 570. Data represent means ± SD of three independent experiments (**C** and **D**). $^{**}P < 0.01$ via a paired Student's *t*-test (for comparisons between 4T1 cells on $Col3^{+/+}$ and $Col3^{-/-}$ fibroblasts; **C**); $^{*}P < 0.05$, $^{**}P < 0.01$ via one-way analysis of variance, followed by Tukey post hoc test (for comparisons between Col3, Col1/3, and Col1; **D**). Original magnification, ×10 (**A** and **B**).

production was limited to fibroblasts in late-stage human mammary carcinoma biopsy specimens, assessed by *in situ* hybridization, and that malignant epithelial cells did not contribute to stromal Col3,[60] although it is possible that 4T1 cells do express some fibrillar collagens *in vivo*. As expected, Col3 expression in $Col3^{-/-}$ fibroblasts was not detectable. Consistent with increased fibrillar collagen production in the tumors of $Col3^{+/-}$ mice, there was a trend for increased Col1 expression in cultured $Col3^{-/-}$ compared to $Col3^{+/+}$ fibroblasts. The lack of a more dramatic effect on Col1 levels suggests that the major effect of Col3 was on matrix organization, although temporal changes in Col1 may lead to significant changes at later times. Together, our data indicate that Col3 suppresses a tumor-inciting stroma and provide strong support for the hypothesis that a Col3-deficient microenvironment promotes breast cancer metastasis.

Discussion

We show herein that Col3 suppresses metastatic behavior of triple-negative breast cancer cells *in vitro* and primary tumor growth and metastasis of 4T1 cells *in vivo*. This is in marked contrast to the tumor- and metastases-promoting behavior of the related fibrillar Col1. Furthermore, we define a

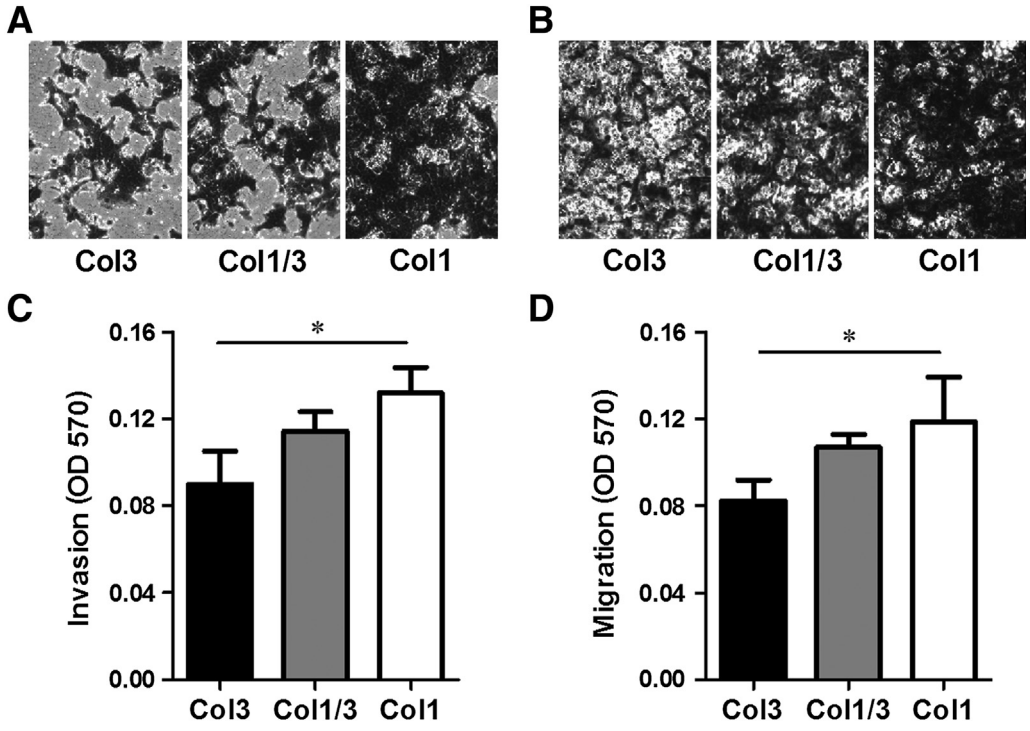

Figure 6 Type III collagen (Col3) impairs murine (4T1) tumor cell invasion and migration. **A** and **C:** 4T1 cells were allowed to invade through a basement membrane–like gel (Matrigel) supplemented with Col3, a 50:50 mixture of Col1/Col3 (Col1/3), or Col1, and through a porous membrane for 16 hours. Cells that had invaded through the gel and the membrane were stained with crystal violet, imaged, and read at OD 570. **B** and **D:** Migration experiments were performed as in **A** and **C**, except no Matrigel was included and instead the collagens were used to coat the membranes. Crystal violet–stained cells appear dark in images **A** and **B**, revealing less invasion and migration in response to a Col3-rich environment. $*P < 0.05$ via one-way analysis of variance, followed by Tukey post hoc test (for comparisons between Col3, Col1/3, and Col1).

previously unreported role for Col3 in regulating matrix organization within the tumor stroma. These data complement our previous finding that Col3 plays a unique role, distinct from Col1, in promoting a regenerative response after cutaneous injury and limiting scar formation,[26] and are consistent with previously published data showing that robust expression of Col3 correlates with improved survival of human breast cancer patients.[32]

Interactions between malignant mammary cells and the surrounding peritumoral stroma play a critical role in mammary tumor progression. Dysregulated ECM dynamics are a defining feature of malignancy, and increased stromal collagen correlates with both increased breast cancer risk and poor prognosis.[4,13–15] In addition, the organization and stiffness of the collagen matrix are key mediators of mammary tumor growth and invasion.[16,18,19,21–24] Aberrant collagen composition, topography, and stiffness can initiate a pro-carcinogenic niche that promotes local tumor invasion and subsequent metastasis through its effects on proliferation, apoptosis, adhesion, invasion, and migration.[1,7,22,24,61,62] Our results show that the collagen from Col3$^{-/-}$ fibroblasts and within tumors of Col3-deficient mice is denser and more highly aligned than in wild-type counterparts (Figure 7) and that this Col3-deficient matrix promotes a tumor-permissive microenvironment (Figures 4, 5, and 6 and Supplemental Figures S2 and S3) that leads to increased primary tumor growth and metastasis (Figure 2). Notably, tumors in Col3$^{+/-}$ mice were found to have significantly increased TACS-3 signatures compared to those from wild-type littermates (Supplemental Figure S4). TACS-3 has been previously shown to correlate with invasive tumor behavior and poor prognosis in women, as well as murine models.[15,16,18,19,24] Given the role of Col3 in regulating collagen alignment, it is possible that Col3 deficiency may also increase stromal stiffness, which is known to promote aggressive breast cancer behavior,[22] although stiffness was not examined in the current study.

Our work defines a role for Col3 in regulating collagen organization both *in vitro* and *in vivo*. Previously, we have shown that Col3 deficiency during cutaneous wound healing results in an increase and persistence of granulation tissue myofibroblasts and a subsequent increase in scar tissue deposition.[26] Similarly, in the tumor microenvironment studied herein, a reduction in Col3 resulted in a robust and aligned SHG signal (Figure 7). Our data also show an increase in density and alignment of α-SMA–positive myofibroblasts in tumors of Col3-haploinsufficient mice. These increased myofibroblast numbers may be secondary to Col3 modulation of myofibroblast recruitment, increased proliferation or attenuated apoptosis (similar to what we show in the tumor cells), or a combination of these processes. Although it is possible that these myofibroblasts are responsible for further remodeling of the Col3-deficient matrix

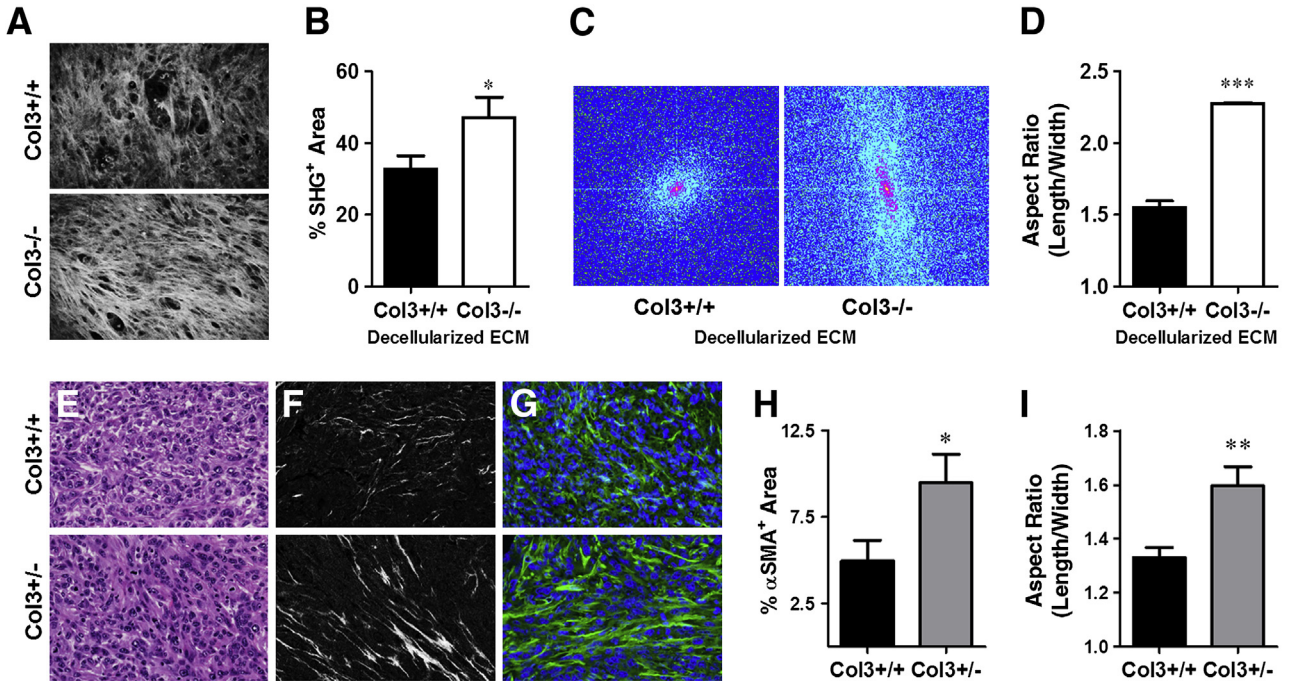

Figure 7 Type III collagen (Col3) deficiency alters collagen matrix in fibroblast-derived matrices and the stromal matrix and increases myofibroblast density and alignment in murine (4T1) tumors. **A:** Second harmonic (SHG) two-photon imaging was used to analyze the fibrillar collagen intensity and organization in $Col3^{+/+}$ and $Col3^{-/-}$ fibroblast-derived matrices. White signal represents collagen fibers. Fibroblasts were isolated from six embryos. **B:** Collagen signal intensity (percentage SHG-positive area; five images taken per individual fibroblast matrix) was analyzed using ImageJ software. **C:** Linearity was analyzed by generating fast Fourier transform (FFT) plots in ImageJ software for each image. Signal that produced a more elongate ellipse represents more aligned, organized fibers. **D:** Linearity was calculated using the FFT plots. **E:** Hematoxylin and eosin sections of 14-day-old tumors (0.5×10^6 cells injected). **F:** SHG imaging was used to visualize the fibrillar collagen in central portions of paraffin-embedded 4T1 tumor sections from $Col3^{+/+}$ and $Col3^{+/-}$ mice. **G:** Sections of 4T1 tumors from $Col3^{+/+}$ and $Col3^{+/-}$ mice (seven per genotype) were stained for α-smooth muscle actin (α-SMA), to label myofibroblasts. Five random images that did not contain tumor edge were taken per tumor. Representative images are shown. Green, α-SMA; blue, DAPI. **H** and **I:** ImageJ software was used to quantify the intensity of α-SMA staining (α-SMA—positive area; **H**) and alignment (**I**). Data represent means ± SEM. $n = 3$ $Col3^{+/+}$ and $Col3^{-/-}$ embryos (**A**). $*P < 0.05$, $**P < 0.01$, and $***P < 0.001$. Original magnification, ×20 (**E**—**G**). ECM, extracellular matrix.

into a more highly aligned matrix, recent data demonstrating that increasing the percentage of Col3 within Col1 gels decreases the density and alignment of fibrillar collagen *in vitro*,[20] paired with the SHG studies presented herein, support an important role for Col3 in modulating fibrillar collagen organization.

The ability of Col3 to decrease collagen network organization likely contributes to its ability to suppress tumor progression[21] and is supported by a significant increase in TACS-3 score development in Col3-deficient ($Col3^{+/-}$) mice. In support of Col3 serving as a gatekeeper to prevent cancer cell escape from the primary tumor, our results from *in vitro* assays reveal significant Col3-dependent reductions in adhesion, invasion, and migration. Similar Col3-dependent suppressive effects on these metastatic processes were found in the human MDA-MB-231 breast cancer cells. Given the relatively modest effect (15% to 40% reduction) in any one process and the much greater (twofold to threefold) effects seen on tumor growth and metastasis *in vivo*, our data suggest that Col3 regulation of breast cancer behavior is complex and multifaceted. Although we did not see a significant increase in tumor cell colonization of Col3-deficient lungs using the tail vein injection assay (Figure 3), it is possible Col3 deficiency in the metastatic niche may still play an important role in regulating metastasis given limitations of this assay. These limitations include limited analysis of the postextravasation process, lack of analysis in the nonpulmonary metastatic niche, and lack of primary tumor presence that may influence the premetastatic microenvironment.[63,64]

Human vascular Ehlers-Danlos syndrome patients have mutations in the *Col3a1* gene and have decreased levels of Col3.[65,66] There are no reports that these patients have an increased risk of cancer, or that they develop more aggressive cancers; however, vascular Ehlers-Danlos syndrome is a rare syndrome and patients have a decreased life span. The risk of cancer in these patients should be studied systematically, because data presented herein suggest that reduced, and not completely absent, tissue Col3 levels may significantly affect breast cancer outcomes. Notably, a large, and growing, population of women at risk for breast cancer may develop an acquired loss of Col3 secondary to smoking, advancing age, the postmenopausal state, and common medications (eg, steroids).[34,54–57,67–69] An age-associated reduction in Col3 in both the lungs (Figure 3A) and in bone[34] (two common sites for breast cancer metastasis) in wild-type mice is consistent with levels seen in the young Col3-haploinsufficient model

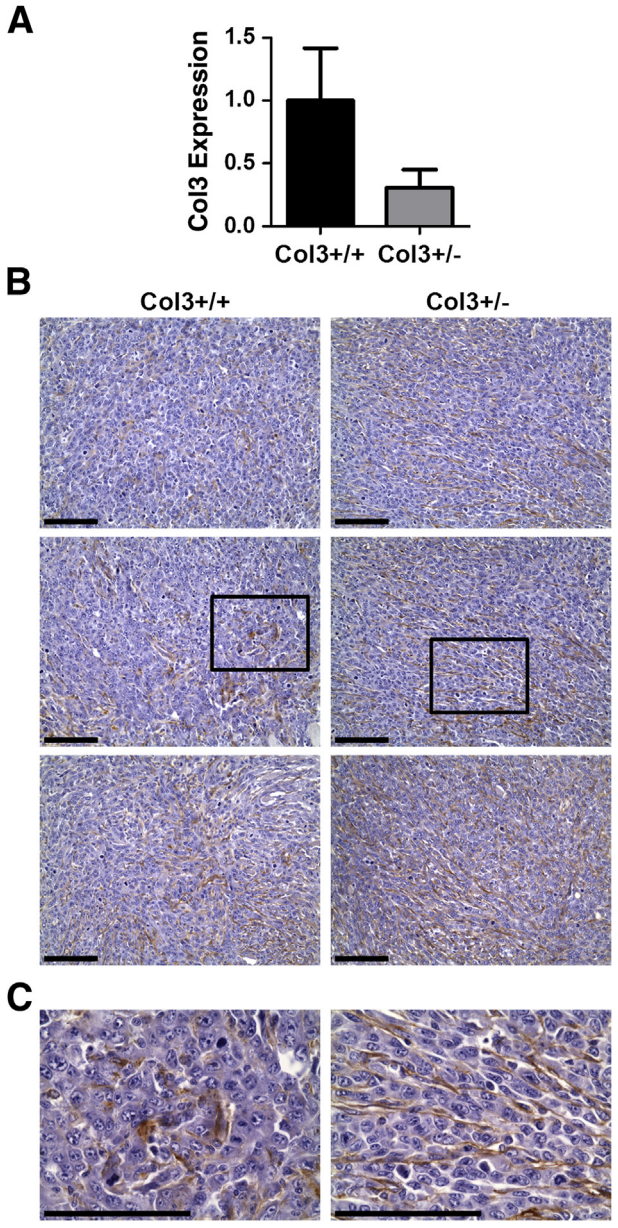

Figure 8 Stromal type III collagen (Col3) density is heterogeneous within murine (4T1) tumors but is localized to the aligned matrix within tumors of $Col3^{+/-}$ mice. **A:** mRNA expression of Col3 in 14-day tumors in $Col3^{+/+}$ and $Col3^{+/-}$ mice. **B:** Images of Col3-stained tumors from $Col3^{+/+}$ and $Col3^{+/-}$ mice showing the heterogeneity in the amount of Col3 staining but the consistent alignment of Col3-containing matrix in tumors of $Col3^{+/-}$ mice. Representative images are from similar regions not containing tumor edge or necrosis. **Boxed areas** are enlarged in **C**. **C:** Images of Col3-stained tumors. $n = 4$ $Col3^{+/+}$ and $Col3^{+/-}$ (**A**). Scale bar = 100 μm (**B** and **C**). Original magnifications: ×20 (**B**); ×60 (**C**).

used in this study, providing further support for this model. Therefore, understanding mechanisms by which Col3 loss leads to increased breast cancer aggressiveness could provide novel targets for intervention in many breast cancer patients.

Although expression of Col3, as a component of a stromal signature, has been linked to improved survival of breast cancer patients, expression of Col3 has yet to be clearly defined as a prognostic marker. In part, this may be due to the enhanced density of myofibroblasts, which may produce Col3. Thus, in Col3-deficient tissue, the evolution of the collagen component of the tumor stroma due to dynamic reciprocity between the ECM, tumor, and stromal cells may ultimately lead to increasing levels of Col3 over time, even though the initial expression of Col3 was low. Col3 production by reactive fibroblasts in malignant breast tumors was demonstrated by a previous study examining collagen expression in late-stage malignant breast tumor biopsy specimens.[60] The dynamic nature of the collagen expression is supported by a lack of significant difference in tumor Col3 at day 14 after orthotopic injection (Figure 8). Spatiotemporal variations in Col3 in the evolving tumor microenvironment may reduce its utility as a prognostic marker at the time of biopsy and may explain why more studies have yet to identify an association between Col3 and prognosis in breast cancer patients. Nonetheless, our data support that Col3 deficiency is a critical contributor to the procarcinogenic microenvironment early in the course of breast cancer through its ability to direct matrix organization that supports metastasis from the primary tumor. In addition, although our data suggest that colonization by metastatic cells is unchanged in Col3-deficient versus wild-type mice, cells that do adhere may have a survival advantage if in a Col3-deficient niche. As such, our identification of a role for Col3 in tumor suppression may aid in identifying patients most at risk for aggressive disease and defining targets for therapy for those with microscopic disease.

Most studies supporting the tumor-permissive properties of a collagen-rich tumor stroma have focused on Col1. Although Col1 clearly plays a role in regulation of tumor behavior, the reference to Col1 as stromal collagen may be unwarranted because it implies similar function of all collagens within the tumor microenvironment. Interestingly, another fibrillar collagen, type V collagen, has been shown to induce breast cancer cell apoptosis.[70] Because of the increasing evidence that the collagen component of the tumor microenvironment plays a key role in directing cancer behavior,[4,13–16,18,19,24] there has been great interest in exploiting antifibrotic agents for use in oncology patients. Notably, our data suggest that nonselective antifibrotic agents that decrease production of Col3 may be detrimental and instead suggest that agents selectively targeting Col1 while preserving Col3 may be more beneficial therapeutically.

Taken together, our data indicate that Col3 plays a previously unrecognized and important role in suppressing primary tumor growth and metastasis in a murine model of triple-negative breast cancer. Clinical relevance is supported by our results using a human breast cancer cell line and previous data suggesting that a stromal response which includes robust expression of Col3, is related to improved clinical outcome in women with breast cancer.[32] We predict that Col3 may have a more global role in regulating cancer

progression and warrants additional investigation. Finally, given its previously defined properties in wound healing, Col3-containing biomaterials applied after excisional biopsy may provide a safe and effective strategy to simultaneously improve healing and limit local recurrence, which has been shown to negatively affect long-term prognosis in breast cancer patients.[71] A better understanding of the mechanisms by which Col3 regulates tumor growth and metastasis may provide novel therapeutic approaches for cancer patients and ensure safety of emerging therapies.

Acknowledgments

We thank Yanjian Wang for technical assistance, Dr. James Monslow for assistance with fast Fourier transform analysis and immunohistology, Dr. Gordon Ruthel for assistance with second harmonic microscopy (performed at the University of Pennsylvania School of Veterinary Medicine Imaging Core), and Dr. Leslie King for critically reviewing and editing the manuscript.

Supplemental Data

Supplemental material for this article can be found at *http://dx.doi.org/10.1016/j.ajpath.2015.01.029*.

References

1. Lu P, Weaver VM, Werb Z: The extracellular matrix: a dynamic niche in cancer progression. J Cell Biol 2012, 196:395−406
2. Dvorak HF, Weaver VM, Tlsty TD, Bergers G: Tumor microenvironment and progression. J Surg Oncol 2011, 103:468−474
3. Radisky ES, Radisky DC: Stromal induction of breast cancer: inflammation and invasion. Rev Endocr Metab Disord 2007, 8: 279−287
4. Lyons TR, O'Brien J, Borges VF, Conklin MW, Keely PJ, Eliceiri KW, Marusyk A, Tan AC, Schedin P: Postpartum mammary gland involution drives progression of ductal carcinoma in situ through collagen and COX-2. Nat Med 2011, 17:1109−1115
5. Tchou J, Conejo-Garcia J: Targeting the tumor stroma as a novel treatment strategy for breast cancer: shifting from the neoplastic cell-centric to a stroma-centric paradigm. Adv Pharmacol 2012, 65: 45−61
6. Gilkes DM, Chaturvedi P, Bajpai S, Wong CC, Wei H, Pitcairn S, Hubbi ME, Wirtz D, Semenza GL: Collagen prolyl hydroxylases are essential for breast cancer metastasis. Cancer Res 2013, 73: 3285−3296
7. Albini A, Mirisola V, Pfeffer U: Metastasis signatures: genes regulating tumor-microenvironment interactions predict metastatic behavior. Cancer Metastasis Rev 2008, 27:75−83
8. Luparello C: Aspects of collagen changes in breast cancer. J Carcinog Mutagen 2013, S13:007
9. Lourenco GJ, Cardoso-Filho C, Goncales NS, Shinzato JY, Zeferino LC, Nascimento H, Costa FF, Gurgel MS, Lima CS: A high risk of occurrence of sporadic breast cancer in individuals with the 104NN polymorphism of the COL18A1 gene. Breast Cancer Res Treat 2006, 100:335−338
10. Barsky SH, Rao CN, Grotendorst GR, Liotta LA: Increased content of type V collagen in desmoplasia of human breast carcinoma. Am J Pathol 1982, 108:276−283
11. Robledo T, Arriaga-Pizano L, Lopez-Perez M, Salazar EP: Type IV collagen induces STAT5 activation in MCF7 human breast cancer cells. Matrix Biol 2005, 24:469−477
12. Iyengar P, Espina V, Williams TW, Lin Y, Berry D, Jelicks LA, Lee H, Temple K, Graves R, Pollard J, Chopra N, Russell RG, Sasisekharan R, Trock BJ, Lippman M, Calvert VS, Petricoin EF 3rd, Liotta L, Dadachova E, Pestell RG, Lisanti MP, Bonaldo P, Scherer PE: Adipocyte-derived collagen VI affects early mammary tumor progression in vivo, demonstrating a critical interaction in the tumor/stroma microenvironment. J Clin Invest 2005, 115:1163−1176
13. Kakkad SM, Solaiyappan M, Argani P, Sukumar S, Jacobs LK, Leibfritz D, Bhujwalla ZM, Glunde K: Collagen I fiber density increases in lymph node positive breast cancers: pilot study. J Biomed Opt 2012, 17:116017
14. Maskarinec G, Pagano IS, Little MA, Conroy SM, Park SY, Kolonel LN: Mammographic density as a predictor of breast cancer survival: the multiethnic cohort. Breast Cancer Res 2013, 15:R7
15. Provenzano PP, Inman DR, Eliceiri KW, Knittel JG, Yan L, Rueden CT, White JG, Keely PJ: Collagen density promotes mammary tumor initiation and progression. BMC Med 2008, 6:11
16. Conklin MW, Eickhoff JC, Riching KM, Pehlke CA, Eliceiri KW, Provenzano PP, Friedl A, Keely PJ: Aligned collagen is a prognostic signature for survival in human breast carcinoma. Am J Pathol 2011, 178:1221−1232
17. Ajeti V, Nadiarnykh O, Ponik SM, Keely PJ, Eliceiri KW, Campagnola PJ: Structural changes in mixed Col I/Col V collagen gels probed by SHG microscopy: implications for probing stromal alterations in human breast cancer. Biomed Opt Express 2011, 2: 2307−2316
18. Provenzano PP, Eliceiri KW, Campbell JM, Inman DR, White JG, Keely PJ: Collagen reorganization at the tumor-stromal interface facilitates local invasion. BMC Med 2006, 4:38
19. Bredfeldt JS, Liu Y, Conklin MW, Keely PJ, Mackie TR, Eliceiri KW: Automated quantification of aligned collagen for human breast carcinoma prognosis. J Pathol Inform 2014, 5:28. eCollection 2014
20. Tilbury K, Lien CH, Chen SJ, Campagnola PJ: Differentiation of Col I and Col III isoforms in stromal models of ovarian cancer by analysis of second harmonic generation polarization and emission directionality. Biophys J 2014, 106:354−365
21. Maller O, Hansen KC, Lyons TR, Acerbi I, Weaver VM, Prekeris R, Tan AC, Schedin P: Collagen architecture in pregnancy-induced protection from breast cancer. J Cell Sci 2013, 126:4108−4110
22. Levental KR, Yu H, Kass L, Lakins JN, Egeblad M, Erler JT, Fong SF, Csiszar K, Giaccia A, Weninger W, Yamauchi M, Gasser DL, Weaver VM: Matrix crosslinking forces tumor progression by enhancing integrin signaling. Cell 2009, 139:891−906
23. Lopez JI, Kang I, You WK, McDonald DM, Weaver VM: In situ force mapping of mammary gland transformation. Integr Biol (Camb) 2011, 3:910−921
24. Conklin MW, Keely PJ: Why the stroma matters in breast cancer: insights into breast cancer patient outcomes through the examination of stromal biomarkers. Cell Adh Migr 2012, 6:249−260
25. Liu X, Wu H, Byrne M, Krane S, Jaenisch R: Type III collagen is crucial for collagen I fibrillogenesis and for normal cardiovascular development. Proc Natl Acad Sci U S A 1997, 94: 1852−1856
26. Volk SW, Wang Y, Mauldin EA, Liechty KW, Adams SL: Diminished type III collagen promotes myofibroblast differentiation and increases scar deposition in cutaneous wound healing. Cells Tissues Organs 2011, 194:25−37
27. Dvorak HF: Tumors: wounds that do not heal: similarities between tumor stroma generation and wound healing. N Engl J Med 1986, 315:1650−1659
28. Rybinski B, Franco-Barraza J, Cukierman E: The wound healing, chronic fibrosis, and cancer progression triad. Physiol Genomics 2014, 46:223−244

29. Mehner C, Radisky DC: Triggering the landslide: the tumor-promotional effects of myofibroblasts. Exp Cell Res 2013, 319: 1657–1662
30. Yamashita M, Ogawa T, Zhang X, Hanamura N, Kashikura Y, Takamura M, Yoneda M, Shiraishi T: Role of stromal myofibroblasts in invasive breast cancer: stromal expression of alpha-smooth muscle actin correlates with worse clinical outcome. Breast Cancer 2012, 19: 170–176
31. Atula S, Grenman R, Syrjanen S: Fibroblasts can modulate the phenotype of malignant epithelial cells in vitro. Exp Cell Res 1997, 235:180–187
32. Beck AH, Espinosa I, Gilks CB, van de Rijn M, West RB: The fibromatosis signature defines a robust stromal response in breast carcinoma. Lab Invest 2008, 88:591–601
33. Committee for the Update of the Guide for the Care and Use of Laboratory Animals; National Research Council: Guide for the Care and Use of Laboratory Animals: Eighth Edition. Washington, DC, National Academies Press, 2011
34. Volk SW, Shah SR, Cohen AJ, Wang Y, Brisson BK, Vogel LK, Hankenson KD, Adams SL: Type III collagen regulates osteoblastogenesis and the quantity of trabecular bone. Calcif Tissue Int 2014, 94:621–631
35. Aslakson CJ, Miller FR: Selective events in the metastatic process defined by analysis of the sequential dissemination of subpopulations of a mouse mammary tumor. Cancer Res 1992, 52: 1399–1405
36. Peng H, Talebzadeh-Farrooji M, Osborne MJ, Prokop JW, McDonald PC, Karar J, Hou Z, He M, Kebebew E, Orntoft T, Herlyn M, Caton AJ, Fredericks W, Malkowicz B, Paterno CS, Carolin AS, Speicher DW, Skordalakes E, Huang Q, Dedhar S, Borden KL, Rauscher FJ 3rd: LIMD2 is a small LIM-only protein overexpressed in metastatic lesions that regulates cell motility and tumor progression by directly binding to and activating the integrin-linked kinase. Cancer Res 2014, 74:1390–1403
37. Egunsola AT, Zawislak CL, Akuffo AA, Chalmers SA, Ewer JC, Vail CM, Lombardo JC, Perez DN, Kurt RA: Growth, metastasis, and expression of CCL2 and CCL5 by murine mammary carcinomas are dependent upon Myd88. Cell Immunol 2012, 272:220–229
38. Leustik M, Doran S, Bracher A, Williams S, Squadrito GL, Schoeb TR, Postlethwait E, Matalon S: Mitigation of chlorine-induced lung injury by low-molecular-weight antioxidants. Am J Physiol Lung Cell Mol Physiol 2008, 295:L733–L743
39. Santos AM, Jung J, Aziz N, Kissil JL, Pure E: Targeting fibroblast activation protein inhibits tumor stromagenesis and growth in mice. J Clin Invest 2009, 119:3613–3625
40. Beacham DA, Amatangelo MD, Cukierman E: Preparation of extracellular matrices produced by cultured and primary fibroblasts. Curr Protoc Cell Biol 2007. Chapter 10:Unit 10.9
41. Otranto M, Sarrazy V, Bonte F, Hinz B, Gabbiani G, Desmouliere A: The role of the myofibroblast in tumor stroma remodeling. Cell Adh Migr 2012, 6:203–219
42. Olsen AL, Bloomer SA, Chan EP, Gaca MD, Georges PC, Sackey B, Uemura M, Janmey PA, Wells RG: Hepatic stellate cells require a stiff environment for myofibroblastic differentiation. Am J Physiol Gastrointest Liver Physiol 2011, 301:G110–G118
43. Tang SY, Monslow J, Todd L, Lawson J, Pure E, FitzGerald GA: Cyclooxygenase-2 in endothelial and vascular smooth muscle cells restrains atherogenesis in hyperlipidemic mice. Circulation 2014, 129:1761–1769
44. Zhang K, Corsa CA, Ponik SM, Prior JL, Piwnica-Worms D, Eliceiri KW, Keely PJ, Longmore GD: The collagen receptor discoidin domain receptor 2 stabilizes SNAIL1 to facilitate breast cancer metastasis. Nat Cell Biol 2013, 15:677–687
45. Miller FR, Miller BE, Heppner GH: Characterization of metastatic heterogeneity among subpopulations of a single mouse mammary tumor: heterogeneity in phenotypic stability. Invasion Metastasis 1983, 3:22–31
46. Stevenson K, Kucich U, Whitbeck C, Levin RM, Howard PS: Functional changes in bladder tissue from type III collagen-deficient mice. Mol Cell Biochem 2006, 283:107–114
47. Briest W, Cooper TK, Tae HJ, Krawczyk M, McDonnell NB, Talan MI: Doxycycline ameliorates the susceptibility to aortic lesions in a mouse model for the vascular type of Ehlers-Danlos syndrome. J Pharmacol Exp Ther 2011, 337:621–627
48. Deak SB, Glaug MR, Pierce RA, Bancila E, Amenta P, Mackenzie JW, Greco RS, Boyd CD: Desmoplasia in benign and malignant breast disease is characterized by alterations in level of mRNAs coding for types I and III procollagen. Matrix 1991, 11:252–258
49. Mori S, Kiuchi S, Ouchi A, Hase T, Murase T: Characteristic expression of extracellular matrix in subcutaneous adipose tissue development and adipogenesis: comparison with visceral adipose tissue. Int J Biol Sci 2014, 10:825–833
50. Duan F, Simeone S, Wu R, Grady J, Mandoiu I, Srivastava PK: Area under the curve as a tool to measure kinetics of tumor growth in experimental animals. J Immunol Methods 2012, 382: 224–228
51. Parra ER, Bielecki LC, Ribeiro JM, Andrade Balsalobre F, Teodoro WR, Capelozzi VL: Association between decreases in type V collagen and apoptosis in mouse lung chemical carcinogenesis: a preliminary model to study cancer cell behavior. Clinics (Sao Paulo) 2010, 65:425–432
52. Kelley J, Chrin L, Coflesky JT, Evans JN: Localization of collagen in the rat lung: biochemical quantitation of types I and III collagen in small airways, vessels, and parenchyma. Lung 1989, 167: 313–322
53. Hance AJ, Bradley K, Crystal RG: Lung collagen heterogeneity: synthesis of type I and type III collagen by rabbit and human lung cells in culture. J Clin Invest 1976, 57:102–111
54. Takeda K, Gosiewska A, Peterkofsky B: Similar, but not identical, modulation of expression of extracellular matrix components during in vitro and in vivo aging of human skin fibroblasts. J Cell Physiol 1992, 153:450–459
55. Varani J, Dame MK, Rittie L, Fligiel SE, Kang S, Fisher GJ, Voorhees JJ: Decreased collagen production in chronologically aged skin: roles of age-dependent alteration in fibroblast function and defective mechanical stimulation. Am J Pathol 2006, 168: 1861–1868
56. Medugorac I: Collagen type distribution in the mammalian left ventricle during growth and aging. Res Exp Med (Berl.) 1982, 180: 255–262
57. Benatti BB, Silverio KG, Casati MZ, Sallum EA, Nociti FH Jr: Influence of aging on biological properties of periodontal ligament cells. Connect Tissue Res 2008, 49:401–408
58. Jaalouk DE, Lammerding J: Mechanotransduction gone awry. Nat Rev Mol Cell Biol 2009, 10:63–73
59. Pouliot N, Pearson HB, Burrows A: Investigating metastasis using in vitro platforms. Edited by Jandial R. Metastatic Cancer: Clinical and Biological Perspectives. Austin, TX, Landes Bioscience, 2013
60. Kauppila S, Stenback F, Risteli J, Jukkola A, Risteli L: Aberrant type I and type III collagen gene expression in human breast cancer in vivo. J Pathol 1998, 186:262–268
61. van't Veer LJ, Dai H, van de Vijver MJ, He YD, Hart AA, Mao M, Peterse HL, van der Kooy K, Marton MJ, Witteveen AT, Schreiber GJ, Kerkhoven RM, Roberts C, Linsley PS, Bernards R, Friend SH: Gene expression profiling predicts clinical outcome of breast cancer. Nature 2002, 415:530–536
62. Ramaswamy S, Ross KN, Lander ES, Golub TR: A molecular signature of metastasis in primary solid tumors. Nat Genet 2003, 33:49–54
63. Francia G, Cruz-Munoz W, Man S, Xu P, Kerbel RS: Mouse models of advanced spontaneous metastasis for experimental therapeutics. Nat Rev Cancer 2011, 11:135–141
64. Rashid OM, Nagahashi M, Ramachandran S, Dumur CI, Schaum JC, Yamada A, Aoyagi T, Milstien S, Spiegel S, Takabe K: Is tail vein

injection a relevant breast cancer lung metastasis model? J Thorac Dis 2013, 5:385–392
65. Byers PH, Holbrook KA, McGillivray B, MacLeod PM, Lowry RB: Clinical and ultrastructural heterogeneity of type IV Ehlers-Danlos syndrome. Hum Genet 1979, 47:141–150
66. Pepin M, Schwarze U, Superti-Furga A, Byers PH: Clinical and genetic features of Ehlers-Danlos syndrome type IV, the vascular type. N Engl J Med 2000, 342:673–680
67. Luther F, Saino H, Carter DH, Aaron JE: Evidence for an extensive collagen type III/VI proximal domain in the rat femur, I: diminution with ovariectomy. Bone 2003, 32:652–659
68. Oishi Y, Fu ZW, Ohnuki Y, Kato H, Noguchi T: Molecular basis of the alteration in skin collagen metabolism in response to in vivo dexamethasone treatment: effects on the synthesis of collagen type I and III, collagenase, and tissue inhibitors of metalloproteinases. Br J Dermatol 2002, 147:859–868
69. Knuutinen A, Kokkonen N, Risteli J, Vahakangas K, Kallioinen M, Salo T, Sorsa T, Oikarinen A: Smoking affects collagen synthesis and extracellular matrix turnover in human skin. Br J Dermatol 2002, 146:588–594
70. Luparello C, Sirchia R: Type V collagen regulates the expression of apoptotic and stress response genes by breast cancer cells. J Cell Physiol 2005, 202:411–421
71. Donker M, Litiere S, Werutsky G, Julien JP, Fentiman IS, Agresti R, Rouanet P, de Lara CT, Bartelink H, Duez N, Rutgers EJ, Bijker N: Breast-conserving treatment with or without radiotherapy in ductal carcinoma in situ: 15-year recurrence rates and outcome after a recurrence, from the EORTC 10853 randomized phase III trial. J Clin Oncol 2013, 31:4054–4059